IEEE Access
Multidisciplinary | Rapid Review | Open Access Journal

Received 20 March 2023, accepted 5 April 2023, date of publication 11 April 2023, date of current version 18 April 2023.

Digital Object Identifier 10.1109/ACCESS.2023.3266421

RESEARCH ARTICLE

An Efficient Primal-Dual Interior-Point Algorithm for Volt/VAR Optimization in Rectangular Voltage Coordinates

H. MATAIFA, S. KRISHNAMURTHY, (Member, IEEE), AND C. KRIGER
Department of Electrical, Electronic and Computer Engineering, Cape Peninsula University of Technology, Bellville, Cape Town 7535, South Africa
Corresponding author: H. Mataifa (mataifah@cput.ac.za)

This work was supported in part by Deutscher Akademischer Austausch Dienst (DAAD)/National Research Foundation (NRF) under Grant DAAD180213312673, in part by NRF Thuthuka under Grant 138177 and Grant TTK210329591306, and in part by the Eskom Tertiary Education Support Program (TESP) and the Eskom Power Plant Engineering Institute (EPPEI).

ABSTRACT Security and reliability of electrical power supply has become indispensable to modern society, and the system operator is challenged to manage the increasingly complex modern power system in a manner that ensures the expected reliability and security of system operation. In this context, Volt/VAR optimization (VVO) plays a key role in the efficient delivery of power through the transmission system, contributing significantly to the security, reliability, quality and economy of system operation. This article presents the design and implementation of an efficient primal-dual interior-point algorithm for the solution of the VVO problem. The primal-dual interior-point method combines efficient constraint handling by means of logarithmic barrier functions, Lagrangian theory of optimization, and the Newton method to constitute one of the most efficient deterministic algorithms for large-scale nonlinear optimization. The developed algorithm also incorporates the efficient Newton-Raphson load flow computation, which ensures that the solution is feasible with respect to the power flow balance equations at each iteration of the VVO algorithm. Both the VVO and Newton-Raphson load flow problems are formulated in the rectangular coordinates of system voltages. This is a departure from most researchers, who make use of the polar formulation, and adds considerably to the efficiency of the developed algorithm. The efficiency and effectiveness of the developed algorithm has been demonstrated by means of case studies performed on the 6-bus and IEEE 14-bus, 30-bus and 118-bus test systems, which have been selected to analyse the computational efficiency and scalability of the algorithm as it is applied to systems of various sizes. The extensive analyses that have been conducted reveal the developed primal-dual interior-point algorithm's effectiveness and efficiency, particularly in being able to successfully solve the VVO problem for systems of widely varying sizes without disproportionate increase in computational cost or deterioration in the quality of the results. The developed algorithm exhibits characteristics of fast convergence, high efficiency, and scalability to large-scale problems.

INDEX TERMS Volt/VAR optimization, reactive power/voltage control, primal-dual interior-point method, optimal power flow, Newton's method, Newton-Raphson load flow, Lagrange multiplier method, rectangular voltage coordinates.

I. INTRODUCTION

The electric power system is arguably one of the most complex engineering systems in existence. For the majority of the world population (and especially the developed world), reliable electrical power supply has become an indispensable daily commodity, the prolonged unavailability of which causes enough disruption to essential public (and private) services and normal daily activities to be considered practically intolerable. To be able to deliver electric power

The associate editor coordinating the review of this manuscript and approving it for publication was Ahmed A. Zaki Diab.

with the required high reliability and security, whilst being economical, planning and operational strategies have been developed over the decades by means of which the system can be operated optimally as far as practicable. These strategies are collectively referred to as Optimal Power Flow (OPF).

The general OPF problem was first formulated in the early 1960s by Carpentier [1], and has since then developed into a sophisticated and indispensable tool for all aspects of power system planning and operation, both in the traditional and deregulated electricity market contexts. Key developments in the treatment of the OPF problem over the years have been presented in a number of review articles, some notable ones being [2], [3], [4], [5], [6], [7], [8], [9], [10], [11], [12], [13], [14], [15], [16]. Gradient-based techniques constituted the first approaches applied to the algorithmic solution for the OPF problem [17], [18], [19]. Over the years, a variety of solution techniques have been explored and developed, falling into two main categories, commonly referred to as classical/conventional or deterministic methods, and heuristic/non-conventional or non-deterministic methods. The category of classical optimization methods includes a variety of gradient-based methods (e.g. reduced-gradient, generalized reduced-gradient, conjugate-gradient, Newton and quasi-Newton methods), and local-approximation methods such as sequential linear programming (SLP) and sequential quadratic programming (SQP). Heuristic optimization methods encompass genetic algorithm, evolutionary programming, particle swarm optimization, fuzzy set theory, and expert systems, among others [20].

The various classical optimization techniques suffer from a number of drawbacks. First-order gradient-based methods, for example, are characterized by slow convergence, and potentially zig-zagging behaviour in the neighbourhood of the optimal solution. Local-approximation techniques (principally SLP and SQP) attempt to reconcile the objectives of (moderate) model complexity and (sufficient) model accuracy by means of iterative model approximation around an operating point (leading to reduced computational effort needed to arrive at the optimal solution), but they are not equally applicable to all problem types, and are particularly not well-suited to handling the stressed operating conditions that modern power systems are quite often subjected to (perhaps due to heavy loading or other phenomena).

The seminal work by Sun et al. [21] that applied Newton's method along with Lagrange multipliers and penalty functions to directly solve the first-order optimality (KKT) conditions for the OPF problem constituted a significant step in the development of efficient methods for solving the large-scale nonlinear OPF problem, although with the major drawback of the approach being the difficulty of identifying the binding inequality constraints at the optimal solution. A class of techniques that uses a similar approach is interior-point methods (IPM), whose origins can be traced back to the barrier methods worked on by Frisch in the 1950s [22], and further developed by Fiacco and McCormick in the 1960s [23]. But the more recent development of IPMs is closely connected with the work of Karmarkar [24], whose discovery of their superior convergence characteristics relative to the Simplex method for linear programming (LP) led to a resurgence in interest for this once-sidelined class of optimization methods, not only for LP, but also for general nonlinear programming (NLP) problems [25]. Interior-point methods possess a number of characteristics that make them particularly attractive for application to large-scale nonlinear optimization, such as fast convergence, and effective handling of inequality constraints by means of logarithmic barrier functions.

An important OPF formulation is the Volt/VAR optimization (VVO) problem, which is primarily concerned with the optimal coordinated dispatch of voltage-regulating devices and reactive power sources so as to maintain a secure voltage profile, thereby enhancing system security, and improving system economy by minimizing system losses [26]. Optimal reactive power dispatch (as it is otherwise referred to) plays a key role in the efficient transfer of real power, especially in the bulk power transmission system, and contributes significantly to the security, reliability, quality and economy of power system operation [27].

In this article, an interior-point method, precisely the primal-dual interior-point method (PDIPM), is used as the basis for developing an efficient Volt/VAR optimization algorithm, which makes use of the rectangular representation of the system voltages, both for the Volt/VAR optimization and the (Newton-Raphson-based) load flow computation (which forms part of the optimization algorithm). The rationale behind this choice is motivated later in the article. Several case studies based on IEEE test systems of various sizes are conducted to evaluate the efficiency of the developed algorithm. The key contributions of the work presented in this article include:

- Development and implementation of an efficient Newton-Raphson load flow algorithm in the rectangular coordinate representation of the system voltages
- Development and implementation of an efficient primal-dual interior-point algorithm for Volt/VAR optimization (PDIPM-VVO), formulated in rectangular coordinates, which incorporates the rectangular-coordinate Newton-Raphson load flow computation
- Comprehensive performance analysis of the developed PDIPM-VVO algorithm, focusing on the quality of the solution (in terms of the magnitude of real power loss percentage reduction and the voltage profile improvement) and the computational efficiency of the algorithm (in terms of the required number of iterations and runtime)
- Demonstrating the scalability of the developed algorithm by analysing its performance for test systems ranging in size from 3-bus to 118-bus system

An outline of the article is as follows. Section II presents the problem formulation for the Volt/VAR optimization problem in rectangular coordinates of the system voltages.

The Newton-Raphson load flow computation is then briefly discussed in Section III before presenting the developed primal-dual interior-point algorithm for Volt/VAR optimization in section IV. Case studies are then presented in section V to analyse the performance of the developed algorithm. Section VI concludes the article with a summary of the key points and results from the article.

II. VOLT/VAR OPTIMIZATION PROBLEM FORMULATION IN RECTANGULAR COORDINATES

Mathematically, Volt/VAR optimization is formulated as a constrained nonlinear optimization problem, intended to minimize a scalar objective function subject to equality and inequality constraints [28]. The main elements of the problem formulation, which need to be specified and defined appropriately, are the system (state and control) variables, the objective(s) of optimization, and the (equality and inequality) constraints. Each of these elements is briefly outlined below, before the full statement of the problem is presented.

A. OBJECTIVES

The primary objective of Volt/VAR optimization is to facilitate the maintenance of network voltage profile within the predetermined nominal range, and at the same time optimize network reactive power dispatch so as to enhance the economical operation of the power system. Key objectives considered in the framework of Volt/VAR optimization are [20]:

- Active power loss minimization
- Reactive power loss minimization
- Voltage profile improvement (e.g. minimization of bus voltage deviation from nominal values)
- Voltage stability maximization
- Minimization of control effort to achieve a desired system operating state

The problem may be formulated to have a single objective or multiple objectives. The active power loss minimization and voltage profile improvement objectives are considered in this study.

B. SYSTEM VARIABLES

System variables can be classified into two types: *state* (dependent) variables and *control* (independent) variables. State variables include [29]:

- Load bus voltage magnitudes
- Load and generator bus phase angles
- Slack bus real power output
- Generator reactive power outputs
- Line flows

Control variables can in turn be classified into those derived from voltage-regulating devices, and those derived from reactive power sources, and include [30]:

- Generator terminal voltage magnitudes
- Under-Load Tap-Changing (ULTC) transformer tap settings
- Shunt capacitors and reactors
- Flexible AC Transmission System (FACTS) devices
- Distributed Generation (DG).

Some of these variables are continuous, others are discrete. A complete and most accurate formulation of the VVO problem would thus be a Mixed Integer Nonlinear Programming (MINLP) problem formulation [31]. Such a problem formulation, although being very accurate (a desirable characteristic), is also computationally intensive, especially for a large-scale system.

C. SYSTEM CONSTRAINTS

The Volt/VAR optimization problem is solved subject to both (generally nonlinear) equality and inequality constraints, which encompass operational and functional-type constraints. The main equality constraints are the bus active and reactive power balance equations, but may also include such constraints as voltage magnitude and/or phase angle imposed or required to be of a specified value at a given bus.

Inequality constraints are of two types: operational constraints that apply to the power system state variables, needed to ensure the secure operation of the system, and physical limits on the operating range of values for the control variables [32]. Limits in the form of inequality constraints are typically imposed on each of the following:

- Generator reactive power outputs
- Bus voltage magnitudes
- Shunt reactive power compensation device outputs
- Load tap changing transformer tap settings
- Line flows (in terms of either active/reactive power or current)

D. GENERAL DEFINITIONS

Here a few definitions useful in the statement of the problem to be presented in the next sub-section are stated. For a given network, the following sets (of indices) can be defined:

N	*Set of (indices over) all buses in the network.*
G	*Set of generators.*
D	*Set of consumers (loads).*
L	*Set of lines/branches in the network.*

Voltage at bus i is a complex quantity, and can be represented in rectangular form as:

$$\bar{V}_i = e_i + jf_i \quad \forall i \in \mathrm{N} \tag{2.1}$$

where e_i and f_i are the real and imaginary components of the complex voltage respectively, $|\bar{V}_i| = \sqrt{e_i^2 + f_i^2}$, and $\theta = \arctan\left({}^{f_i}/_{e_i}\right)$ are the magnitude and phase angle of the voltage at bus i respectively. The rectangular form of the active (P_i) and reactive (Q_i) power injections at bus i can be expressed as [33]:

$$P_i = G_{ii}\left(e_i^2 + f_i^2\right) + e_i \sum_{j \in L_i} G_{ij}e_j - B_{ij}f_j + f_i \sum_{j \in L_i} G_{ij}f_j + B_{ij}e_j \tag{2.2}$$

$$Q_i = -B_{ii}\left(e_i^2 + f_i^2\right) + f_i \sum_{j\in L_i} G_{ij}e_j - B_{ij}f_j - e_i \sum_{j\in L_i} G_{ij}f_j + B_{ij}e_j \tag{2.3}$$

where G_{ij} and B_{ij} are the real and imaginary components of the ij^{th} element of the bus admittance matrix Y, that is, $Y_{ij} = G_{ij} + jB_{ij}$. L_i is the set of branches (or lines) directly connected to bus i.

The active power losses (P_L) in the transmission system can be expressed as a summation of the losses over all the branches of the network. In rectangular form, this can be derived as [34]:

$$P_L = \sum_{(i,j)\in L} G_{ij}\left[(e_i - e_j)^2 + (f_i - f_j)^2\right] \tag{2.4}$$

The rectangular formulation has the main advantage that for the Volt/VAR optimization problem, the objective and constraint functions are quadratic functions of the bus voltages (as can be deduced from (2.2) – (2.4)), and the Hessian matrices are constant [32]. This turns out to be numerically very efficient for a Newton-based optimization algorithm, and enables direct handling of the strong nonlinearity typical in some power system problems, such as the Volt/VAR optimization problem, while keeping the computational effort moderate.

E. STATEMENT OF THE VOLT/VAR OPTIMIZATION PROBLEM

Based on the components of the problem formulation and the general definitions presented in the preceding subsections, the Volt/VAR optimization problem expressed in the rectangular coordinates of the bus voltages can be stated as [32] and [33]:

$$\min P_L\,(e, f, t) \tag{2.5}$$

subject to:

$$P_i\,(e, f, t) + P_{di} - P_{gi} = 0 \tag{2.6}$$
$$Q_i\,(e, f, t, q) + Q_{di} - q_i - Q_{gi} = 0 \tag{2.7}$$
$$Y_{ij}^2\left[(e_i - e_j)^2 + (f_i - f_j)^2\right] \le \left(I_{ij}^{\max}\right)^2 \tag{2.8}$$
$$\left(V_i^{\min}\right)^2 \le e_i^2 + f_i^2 \le \left(V_i^{\max}\right)^2 \tag{2.9}$$
$$Q_{gi}^{\min} \le Q_{gi} \le Q_{gi}^{\max} \tag{2.10}$$
$$q_i^{\min} \le q_i \le q_i^{\max} \tag{2.11}$$
$$\tau_{ij}^{\min} \le \tau_{ij} \le \tau_{ij}^{\max} \tag{2.12}$$

The mathematical symbols (not yet defined) in the formulation above have the following definitions:

P_{di}/Q_{di}	*Active/reactive power demand at bus i.*
P_{gi}/Q_{gi}	*Active/reactive power generation at bus i.*
I_{ij}	*Current magnitude in branch ij.*
V_i	*Bus voltage magnitude at bus i.*
q_i	*Reactive power compensation at bus i.*
τ_{ij}	*Tap position of ULTC connected in branch ij.*

In the problem formulation stated above (2.5) represents the objective function, which is defined by (2.4). Equations (2.6) and (2.7) are the active and reactive power balance equations, with P_i and Q_i given by (2.2) and (2.3) respectively. Equation (2.8) represents branch flow limits expressed in terms of the maximum current limit, and (2.9) – (2.12) constitute lower and upper bounds on the bus voltage magnitudes, generator reactive power outputs, shunt reactive power compensation, and ULTC transformer tap settings, respectively.

To facilitate the development of the primal-dual interior-point algorithm (PDIPA) to be presented later, the problem formulation can be stated in compact form as the following general nonlinear programming problem [28]:

$$\min \quad f\,(x) \tag{2.13}$$

subject to:

$$g\,(x) = 0 \tag{2.14}$$
$$h\,(x) \le 0 \tag{2.15}$$

where (2.14) represents the equality constraints (2.6) – (2.7), and (2.15) bundles together all the inequality constraints, (2.8) – (2.12).

The developed PDIPA requires the execution of a load flow computation at each iteration of the optimization algorithm. The following section thus briefly discusses the design and implementation of the load flow computation in rectangular coordinates, in line with the problem formulation used in the Volt/VAR optimization.

III. NEWTON-RAPHSON LOAD FLOW COMPUTATION IN RECTANGULAR COORDINATES

The objective of a load flow computation for a power system is to determine the system bus voltages (magnitudes and phase angles) for a given generation, load and network condition, while satisfying active and reactive power balance equations (i.e. sum of active and reactive power injections at each bus, each treated separately, must equal zero) [35]. Other than handling the active and reactive power balance equations, the load flow algorithm does not enforce the satisfaction of any other system constraints (such as limits on bus voltage magnitudes and other state variables), which thus needs to be taken care of as part of the Volt/VAR optimization. Once the system voltages have been determined, other system quantities such as line power flows and system losses can be computed in turn as part of the load flow solution of the system [36].

TABLE 1. Classification of system buses for load flow computation based on specified and unknown variables.

Bus type	Voltage ($\|V\|\angle\delta$)		Real power (P)		Reactive power (Q)	
	Magnitude	Angle	Generation	Load	Generation	Load
Reference/slack/swing	Specified	Specified	Unknown	-	Unknown	-
Generator/PV/regulated	Specified	Unknown	Specified	-	Unknown	-
Load/PQ	Unknown	Unknown	-	Specified	-	Specified

The load flow problem is a nonlinear problem, and a number of methods, most of them iterative, have been developed and applied to it, prominent among them being the Newton-Raphson, Gauss-Seidel, fast-decoupled, and DC load flow methods, all of which are extensively discussed in power system analysis textbooks (see, for example, [37], [38]). The Newton-Raphson method is very popular for its high efficiency, and it forms the basis for the load flow computation in this study.

A load flow computation requires classifying each system bus on the basis of the known and unknown variables at the bus, as detailed in Table 1. All system buses essentially fall broadly into two main categories, depending on whether there is generation at the bus or not. Non-generator buses are referred to as load (or PQ) buses, and the rest are referred to as generator (or PV or regulated) buses. Among generator buses, one bus (possibly more) is designated as the reference bus, which is responsible for setting the reference voltage phase angle for the system, as well as catering for the mismatch between load demand (plus system losses) and scheduled generation. Hence, it is also referred to as the slack bus or swing bus [37].

As can be deduced from Table 1, both the voltage magnitude and voltage phase angle are specified at the reference bus, the voltage magnitude is specified at each generator bus, whereas neither voltage magnitude nor phase angle is specified at load buses. The load flow solution is thus needed to compute voltage magnitudes and phase angles for all load buses, as well as voltage phase angles for (non-slack) generator buses [35].

To develop the Newton-Raphson-based load flow algorithm, a vector of power (ΔP_i, ΔQ_i) and voltage (ΔV_i^2) mismatches is constructed using the following expressions [36]:

$$\begin{aligned}\Delta P_i &= P_i + P_{di} - P_{gi} \\ &= G_{ii}\left(e_i^2 + f_i^2\right) + e_i \sum_{j\in L_i} G_{ij}e_j - B_{ij}f_j \\ &\quad + f_i \sum_{j\in L_i} G_{ij}f_j + B_{ij}e_j + P_{di} - P_{gi} \end{aligned} \tag{3.1}$$

$$\begin{aligned}\Delta Q_i &= Q_i + Q_{di} - q_i - Q_{gi} \\ &= -B_{ii}\left(e_i^2 + f_i^2\right) + f_i \sum_{j\in L_i} G_{ij}e_j - B_{ij}f_j \\ &\quad - e_i \sum_{j\in L_i} G_{ij}f_j + B_{ij}e_j + Q_{di} - q_i - Q_{gi} \end{aligned} \tag{3.2}$$

$$\Delta V_i^2 = V_i^2 - \left(e_i^2 + f_i^2\right) \tag{3.3}$$

Equation (3.1) is the active power (or active power balance) mismatch, and needs to be computed for each bus other than the slack bus. Equation (3.2) is the reactive power mismatch, and needs to be computed for each load bus. Equation (3.3) is the voltage magnitude mismatch, and needs to be computed for each generator bus except for the slack bus, to ensure maintenance of the voltage magnitude set-point at the voltage-regulated (i.e. PV) buses. For a system with n buses, a total of $2(n-1)$ equations are formulated in order to solve for the load-bus voltage magnitudes and phase angles, as well as PV-bus voltage phase angles [39]. The mismatch equations (3.1) – (3.3) have been expressed in rectangular form, as the developed load flow algorithm is based on the rectangular representation of system bus voltages. Incidentally, (3.1) and (3.2) can be recognized as the active and reactive power balance equations, which appear as (2.6) and (2.7) respectively in the Volt/VAR optimization problem formulation. The implication of this is that the Volt/VAR optimization problem formulation need only treat the inequality constraints, equations (2.8) – (2.12), since the equality constraints are accounted for in the load flow computation.

The basic idea of Newton-Raphson-based the load flow computation is to drive the mismatches (otherwise referred to as residues) toward zero in an iterative manner. This is done by application of the Newton method, an iterative procedure for finding the solution to a general nonlinear problem of the form [36]:

$$F(X) = 0 \tag{3.4}$$

which involves generating the Taylor series expansion of $F(X)$ about an initial estimated solution X^0, subjected to a small increment ΔX^0, then taking the first-order approximation of the expansion, valid under certain assumptions (see, for example, [35], for additional information on the Newton method). The resulting first-order model that forms the basis for the Newton-Raphson load flow computation can be expressed as [38]:

$$J(X)\Delta X = -F(X) \tag{3.5}$$

where $F(X)$ is a vector whose elements are based on (3.1) – (3.3) as further discussed shortly, $J(X)$ is the Jacobian of $F(X)$ (i.e. the first-order partial derivatives of $F(X)$ with respect to the system bus voltages), and ΔX is the correction vector to be applied to the variable X (the system bus voltages) in order to drive it towards the load flow

solution, according to equation (3.6).

$$X^{k+1} = X^k + \Delta X^k \tag{3.6}$$

For each i^{th} PQ bus, the mismatch vector (F_{PQ_i}) and the corresponding Jacobian ($J_{PQ_{ij}}$) are given by [36]:

$$F_{PQ_i} = \begin{bmatrix} \Delta P_i \\ \Delta Q_i \end{bmatrix} \tag{3.7}$$

$$J_{PQ_i} = \begin{bmatrix} \frac{\partial \Delta P_i}{\partial e_j} & \frac{\partial \Delta P_i}{\partial f_j} \\ \frac{\partial \Delta Q_i}{\partial e_j} & \frac{\partial \Delta Q_i}{\partial f_j} \end{bmatrix} \tag{3.8}$$

And for each i^{th} PV bus, the mismatch vector (F_{PV_i}) and the corresponding Jacobian (J_{PV_i}) are given by [36]:

$$F_{PV_i} = \begin{bmatrix} \Delta P_i \\ \Delta V_i^2 \end{bmatrix} \tag{3.9}$$

$$J_{PV_i} = \begin{bmatrix} \frac{\partial \Delta P_i}{\partial e_j} & \frac{\partial \Delta P_i}{\partial f_j} \\ \frac{\partial \Delta V_i^2}{\partial e_j} & \frac{\partial \Delta V_i^2}{\partial f_j} \end{bmatrix} \tag{3.10}$$

and the correction vector ΔX_i is given by [36]:

$$\Delta X_i = \begin{bmatrix} \Delta e_i \\ \Delta f_i \end{bmatrix} \tag{3.11}$$

for every bus other than the slack bus. The increment ΔX^k is successively added to the current solution X^k at each iteration until the approximate solution reaches a sufficient level of accuracy. Computation of the elements of the Jacobian based on (3.1) – (3.3) is quite straightforward, but details are not presented here to keep the length of the article reasonable. A flowchart of the Newton-Raphson load flow algorithm is depicted in Fig. 1.

IV. DESCRIPTION OF THE PRIMAL-DUAL INTERIOR-POINT-ALGORITHM FOR VOLT/VAR OPTIMIZATION

The primal-dual interior-point method (PDIPM) effectively combines three key concepts to provide an approach for solving constrained nonlinear optimization problems: (i) handling of inequality constraints by means of logarithmic barrier functions, (ii) application of Lagrangian theory of optimization to the solution of an equality-constrained optimization problem, and (iii) application of the Newton method to solve the resulting unconstrained optimization problem, which can be treated as a general nonlinear problem [32]. The main steps of the technique can be outlined as:

1. Deriving the first-order optimality (KKT) conditions, which in turn comprises the following steps:
   - 1.1. Transforming all inequality constraints into equality constraints by adding a nonnegative slack variable to each inequality constraint
   - 1.2. Implicit handling of the non-negativity condition of slack variables by augmenting each of them to the objective function using a logarithmic barrier function
   - 1.3. Transforming the resulting equality-constrained optimization problem into an unconstrained one using the Lagrangian-multiplier method
   - 1.4. Taking the first-order partial derivatives of the Lagrangian function with respect to the primal and dual variables, and equating them to zero
2. Solving the resulting *perturbed* KKT system using the Newton method

A detailed description of the primal-dual interior-point algorithm is presented in the following sub-sections. The steps of the algorithm are then summarized in the form of a flowchart, presented in Fig. 2.

A. DERIVING THE FIRST-ORDER OPTIMALITY CONDITIONS

As outlined above, the first step in the derivation of the first-order optimality conditions is to transform each inequality constraint into an equality constraint by adding to it a non-negative slack variable (s). Using the general nonlinear programming problem formulation (2.13) – (2.15), this step results in the following form of the problem:

$$\min f(x) \tag{4.1}$$

subject to:

$$g(x) = 0 \tag{4.2}$$

$$h(x) + s = 0 \tag{4.3}$$

$$s \geq 0 \tag{4.4}$$

The next step is to implicitly handle the non-negativity condition of the slack variables (4.4) by augmenting them to the objective function by means of logarithmic barrier functions. This transforms the problem into the following form:

$$\min \quad f(x) - \mu \sum_{i=1}^{p} \ln(s_i) \tag{4.5}$$

subject to:

$$g(x) = 0 \tag{4.6}$$

$$h(x) + s = 0 \tag{4.7}$$

where μ is a positive scalar, referred to as the barrier parameter, which is progressively decreased to zero as the iteration progresses. It has been shown by Fiacco and McCormick [23] that as μ tends to zero, the solution of the problem (4.5) – (4.7), $x(\mu)$, approaches the optimizer $x*$ of the original problem (2.13) – (2.15).

Following the previous step, the problem has been transformed into an equality-constrained optimization problem. The next step is to transform it into an unconstrained optimization problem by constructing the Lagrangian function as a linear combination of the logarithmic barrier-augmented

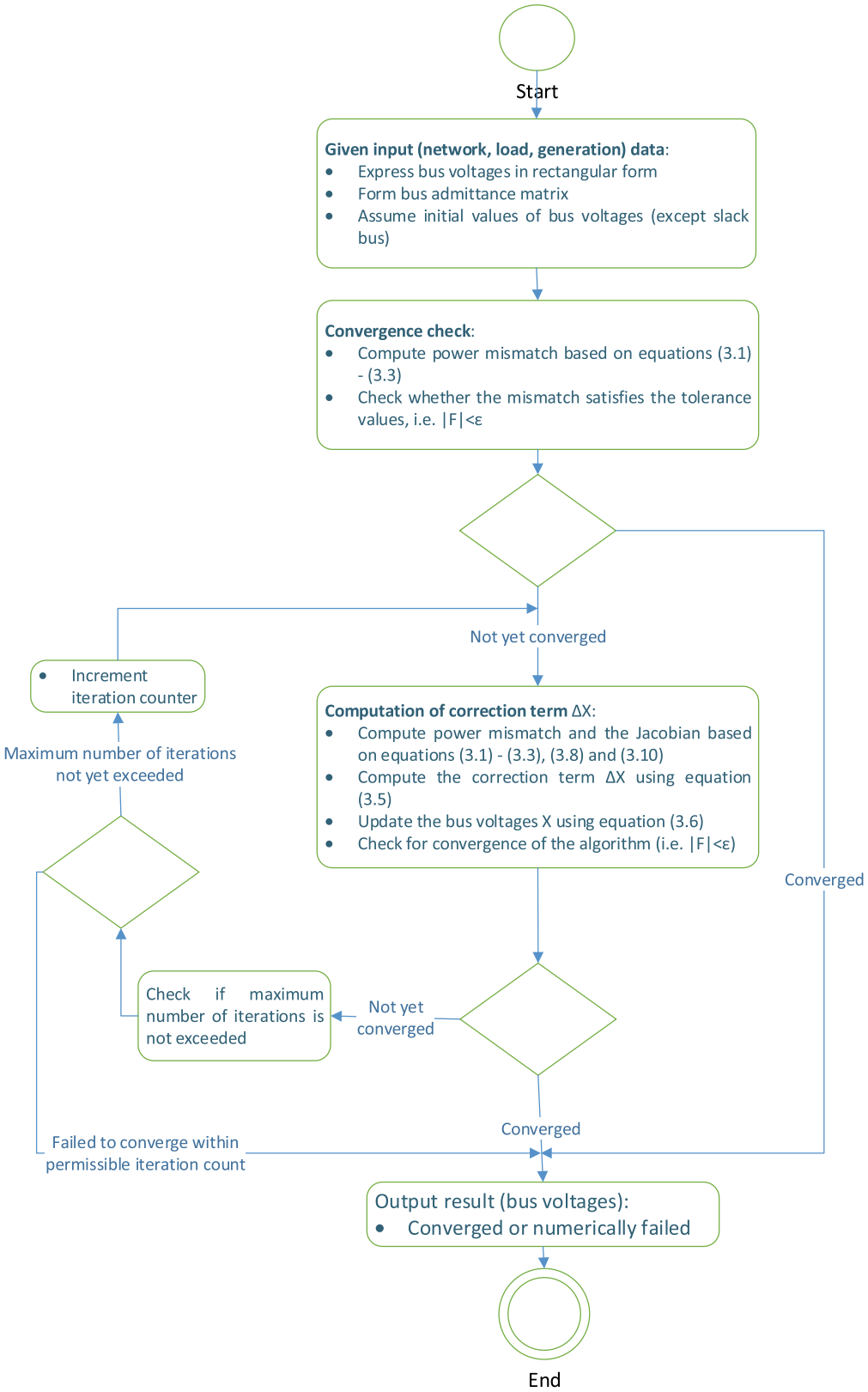

FIGURE 1. Flowchart of the Newton-Raphson load flow algorithm.

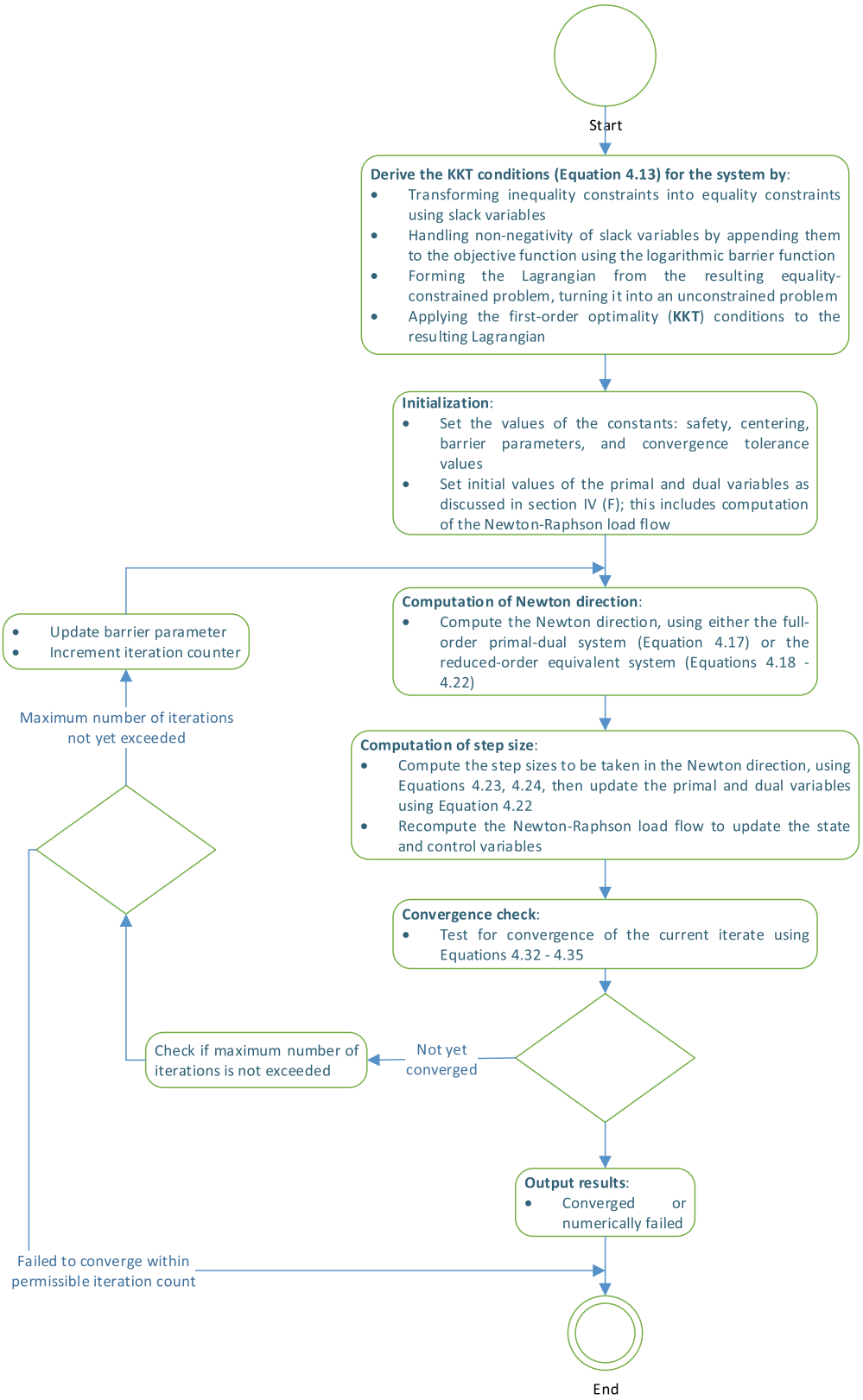

FIGURE 2. Flowchart of the primal-dual interior-point algorithm for VVO.

objective function and the equality constraints, according to the following expression [40]:

$$L_\mu = f(x) - \mu \sum_{i=1}^{p} \ln(s_i) + \lambda_E^T g(x) + \lambda_I^T (h(x) + s) \tag{4.8}$$

where λ_E and λ_I are the Lagrange multipliers for the equality and inequality constraints respectively. The first-order optimality (KKT) conditions of the problem can now be derived by taking the first-order partial derivatives of (4.8) with respect to each of the primal and dual variables (i.e. the variables $x, s, \lambda_E, \lambda_I$), and equating each of them to zero, with the following result [40]:

$$\nabla_x L_\mu = \nabla f(x) + \nabla g^T(x)\lambda_E + \nabla h^T(x)\lambda_I = 0 \tag{4.9}$$
$$\nabla_s L_\mu = -\mu S^{-1} e + \lambda_I = 0 \tag{4.10}$$
$$\nabla_{\lambda_E} L_\mu = g(x) = 0 \tag{4.11}$$
$$\nabla_{\lambda_I} L_\mu = h(x) + s = 0 \tag{4.12}$$

where e is a vector of ones of appropriate length (i.e. $e = [1, 1, \ldots, 1]^T$), S is a diagonal matrix with the slack variables on the diagonal (i.e. $S = diag\left(s_1, s_2, \ldots, s_p\right)$). The KKT conditions (4.9) – (4.12) can be written in a compact form as:

$$F(X) = \begin{bmatrix} \nabla_x L_\mu \\ \nabla_s L_\mu \\ \nabla_{\lambda_E} L_\mu \\ \nabla_{\lambda_I} L_\mu \end{bmatrix} = \begin{bmatrix} \nabla f(x) + \nabla g^T(x)\lambda_E + \nabla h^T(x)\lambda_I \\ S\lambda_I - \mu e \\ g(x) \\ h(x) + s \end{bmatrix} = 0 \tag{4.13}$$

The second row in (4.13) is obtained by multiplying (4.10) by S, which has the advantage (particularly for the Newton method) of decreasing the relative nonlinearity of the primal-dual system near the solution as $s \to 0$ [41].

Equation (4.13) constitutes the KKT conditions that are needed to be derived as the first step in the primal-dual interior-point method. The next step is to solve this system in an iterative process, which involves the following steps [33]:

- Determining the search direction (by the Newton method)
- Determining the step size to be taken in the already computed search direction, then updating the primal and dual variables
- Updating the barrier parameter, which should monotonically be decreased to zero as the iterative process proceeds
- Checking the stopping criteria that indicate the algorithm's convergence to the solution of the problem

B. DETERMINING THE SEARCH DIRECTION BY THE NEWTON METHOD

Computing the search direction for the KKT system based on the Newton method follows a procedure similar to that outlined in section III for the Newton-Raphson load flow algorithm. In this case, (3.5) is applied with $F(X)$ given by (4.13), the Jacobian of the system $J(X)$ and the correction vector ΔX given by (4.14) and (4.15) respectively.

$$J(X) = \begin{bmatrix} \nabla^2_{xx} L_\mu & \nabla^2_{xs} L_\mu & \nabla^2_{x\lambda_E} L_\mu & \nabla^2_{x\lambda_I} L_\mu \\ \nabla^2_{sx} L_\mu & \nabla^2_{ss} L_\mu & \nabla^2_{s\lambda_E} L_\mu & \nabla^2_{s\lambda_I} L_\mu \\ \nabla^2_{\lambda_E x} L_\mu & \nabla^2_{\lambda_E s} L_\mu & \nabla^2_{\lambda_E \lambda_E} L_\mu & \nabla^2_{\lambda_E \lambda_I} L_\mu \\ \nabla^2_{\lambda_I x} L_\mu & \nabla^2_{\lambda_I s} L_\mu & \nabla^2_{\lambda_I \lambda_E} L_\mu & \nabla^2_{\lambda_I \lambda_I} L_\mu \end{bmatrix} = \begin{bmatrix} \nabla^2_{xx} L_\mu & 0 & \nabla g^T(x) & \nabla h^T(x) \\ 0 & \Lambda_I & 0 & S \\ \nabla g(x) & 0 & 0 & 0 \\ \nabla h(x) & I & 0 & 0 \end{bmatrix} \tag{4.14}$$

$$\Delta X = \begin{bmatrix} \Delta x \\ \Delta s \\ \Delta \lambda_E \\ \Delta \lambda_I \end{bmatrix} \tag{4.15}$$

$$\nabla^2_{xx} L_\mu = \nabla^2_{xx} f(x) + \nabla^2_{xx} g^T(x)\lambda_E + \nabla^2_{xx} h^T(x)\lambda_I \tag{4.16}$$

where Λ_I is a diagonal matrix with the Lagrange multiplier vector for the inequality constraints, λ_I, on the diagonal (i.e. $\Lambda_I = diag\left([\lambda_I]\right)$). Equation (4.16) defines the Hessian matrix of the Lagrangian function with respect to the decision variable, $\nabla^2_{xx} L_\mu$, which appears in (4.15). Based on (3.5) and (4.13) – (4.16), the primal-dual system can be expressed as in (4.17). Using elimination and substitution, a reduced-order equivalent system can be derived from (4.17), where Δs is expressed in terms of Δx and $\Delta \lambda_I$ in terms of Δs [41].

$$\begin{bmatrix} \nabla^2_{xx} L_\mu & 0 & \nabla g^T(x) & \nabla h^T(x) \\ 0 & \Lambda_I & 0 & S \\ \nabla g(x) & 0 & 0 & 0 \\ \nabla h(x) & I & 0 & 0 \end{bmatrix} \begin{bmatrix} \Delta x \\ \Delta s \\ \Delta \lambda_E \\ \Delta \lambda_I \end{bmatrix} \cdots = -\begin{bmatrix} \nabla f(x) + \nabla g^T(x)\lambda_E + \nabla h^T(x)\lambda_I \\ S\lambda_I - \mu e \\ g(x) \\ h(x) + s \end{bmatrix} \tag{4.17}$$

Considering the second and fourth rows of equation (4.17), expressions for the slack variable (Δs) and Lagrange multiplier ($\Delta \lambda_I$) mismatches can be derived as:

$$\Delta s = -h(x) - s - \nabla h(x)\Delta x \tag{4.18}$$
$$\Delta \lambda_I = S^{-1}\left(-S\lambda_I + \mu e - \Lambda_I \Delta s\right) \tag{4.19}$$

The reduced-order equivalent system results from substituting (4.19) into the first row of (4.17), simplifying and then combining with the third row of (4.17) to result in:

$$\begin{bmatrix} A & \nabla g^T(x) \\ \nabla g(x) & 0 \end{bmatrix} \begin{bmatrix} \Delta x \\ \Delta \lambda_E \end{bmatrix} = -\begin{bmatrix} B \\ g(x) \end{bmatrix} \tag{4.20}$$
$$A = \nabla^2_{xx} L_\mu + \nabla h^T(x) S^{-1} \Lambda_I \nabla h(x) \tag{4.21}$$
$$B = \nabla_x L_\mu + \nabla h^T(x) S^{-1} \left(\mu e + \Lambda_I h(x)\right) \tag{4.22}$$

TABLE 2. Main dimensions of the test cases.

System	Number of buses	Number of generators	Number of lines	Number of loads
6-bus	6	3	11	3
IEEE 14-bus	14	5	20	11
IEEE 30-bus	30	6	41	21
IEEE 118-bus	118	54	186	99

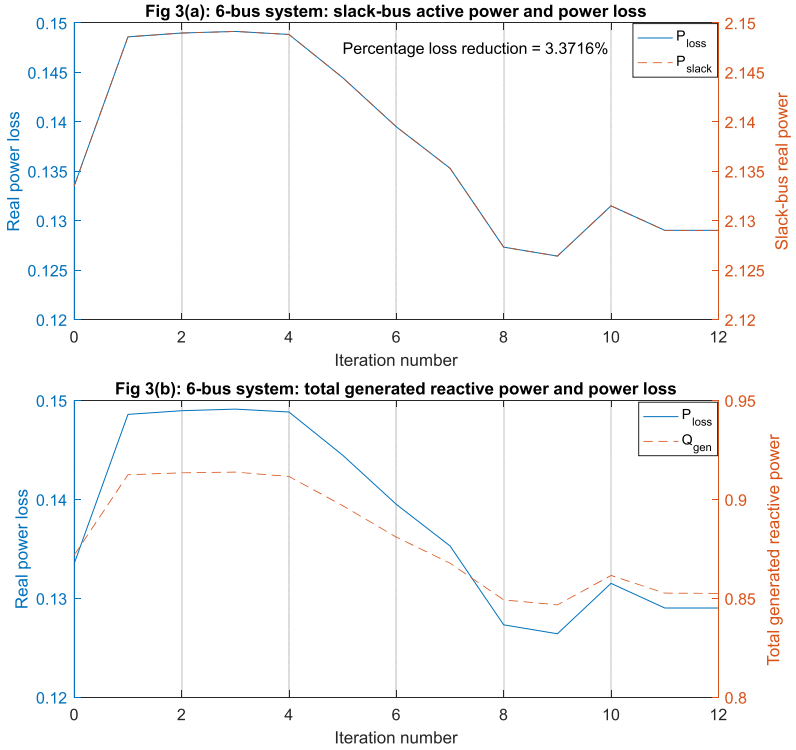

FIGURE 3. 6-bus system comparison of real power loss with slack-bus active power (3a) and with total generated reactive power (3b).

Incidentally, since the Volt/VAR optimization as designed in this study handles only the inequality constraints, as explained in section III, the reduced-order equivalent primal-dual system (4.20) further reduces to:

$$A\Delta x = -B \tag{4.23}$$

Thus, to determine the Newton direction for the primal-dual system (4.17), we can alternatively solve the reduced-order equivalent system (4.21) – (4.23), along with (4.18) and (4.19). The reduction in the order of the system has the advantage of incurring relatively lower computational expense [41].

Once the Newton direction has been computed, a number of other algorithm implementation aspects need to be addressed, specifically [33]:

- Determination of the step length to be taken in the Newton direction
- Adjustment of the barrier parameter
- Checking the convergence of the algorithm
- Initialization of the algorithm parameters

Each of these implementation issues is briefly discussed next.

C. DETERMINING THE STEP LENGTH

Once the Newton direction has been computed as in the previous sub-section, the primal and dual variables are updated according to the following expressions [42]:

$$x^{k+1} = x^k + \alpha_p^k \Delta x^k \tag{4.24}$$

$$s^{k+1} = s^k + \alpha_p^k \Delta s^k \tag{4.25}$$

$$\lambda_I^{k+1} = \lambda_I^k + \alpha_d^k \Delta \lambda_I^k \tag{4.26}$$

$\alpha_p \in (0, 1]$ and $\alpha_d \in (0, 1]$ are the step lengths taken in the Newton direction for the primal and dual spaces respectively, and effectively constitutes incorporating a line search into the Newton method, with the dual objective of advancing the iterates towards optimality while maintaining feasibility (specifically the strict positivity condition of the slack variables and their corresponding dual variables). A commonly used line search method for the step lengths is

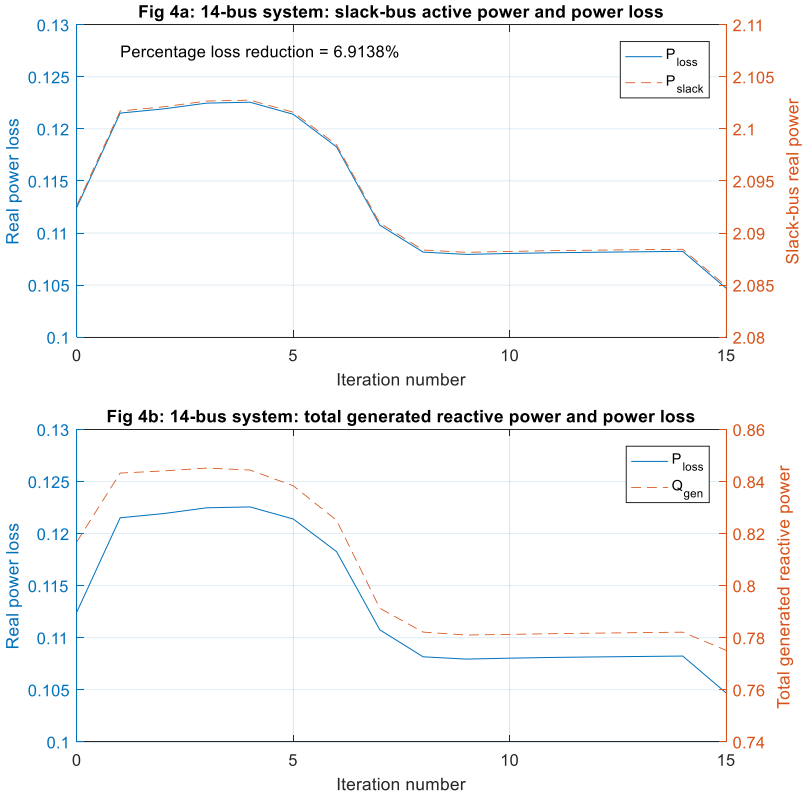

FIGURE 4. 14-bus system comparison of real power loss with slack-bus active power (4a) and with total generated reactive power (4b).

by means of the expressions [32]:

$$\alpha_p = \min\left(1, \zeta \min_{\Delta s_i<0}\left(-\frac{s_i}{\Delta s_i}\right)\right) \tag{4.27}$$

$$\alpha_d = \min\left(1, \zeta \min_{\Delta \lambda_{Ii}<0}\left(-\frac{\lambda_{Ii}}{\Delta \lambda_{Ii}}\right)\right) \tag{4.28}$$

where $\zeta \in (0, 1)$ defines a *safety factor*, intended to ensure strict positivity of the slack variables and their corresponding dual variables. It is commonly set to be as close to unity as possible, to enable taking a sufficiently large step in the Newton direction. A value of $\zeta = 0.9995$ has been used in this study.

It is also worth pointing out that in the case of primal-dual interior-point methods for nonlinear programming, close coupling between the primal and dual variables provides for the possibility of using a common step length adjustment [32], which is then taken as the minimum of the two, that is:

$$\alpha = \min\left(\alpha_p, \alpha_d\right) \tag{4.29}$$

Use of a common step length usually works well provided there isn't a great discrepancy in the magnitudes of the two step lengths, otherwise the convergence characteristics of the algorithm might be adversely impacted [32].

D. DECREASING THE BARRIER PARAMETER

The KKT conditions represented by (4.13) are referred to as the *perturbed* KKT conditions [41], due to the presence of the barrier parameter μ. For the solution of this system to coincide with that of the original problem, a scheme is required to monotonically decrease μ towards zero as the iterations progress. The scheme employed to decrement μ has a significant impact on the convergence characteristics of the algorithm. If decreased too slowly, the number of iterations required for the interior-point algorithm becomes large. If decreased too quickly, some of the slack or dual variables may approach zero prematurely, again slowing down the rate of progress of the iterations [43]. Most (modern) implementations of the interior-point method use an adaptive strategy for updating the barrier parameter, varying it at every iteration as a function of the progress of the algorithm, based on the complementarity gap, that is, the residue of the complementarity constraints:

$$\rho = s^T \lambda_I \tag{4.30}$$

The barrier parameter is adjusted proportionately to the complementarity gap (4.30) according to [32]:

$$\mu^{k+1} = \sigma^k \frac{\rho^k}{2(m+p)} \tag{4.31}$$

where m and p are the numbers of equality and inequality constraints respectively, σ defines a *centering parameter*,

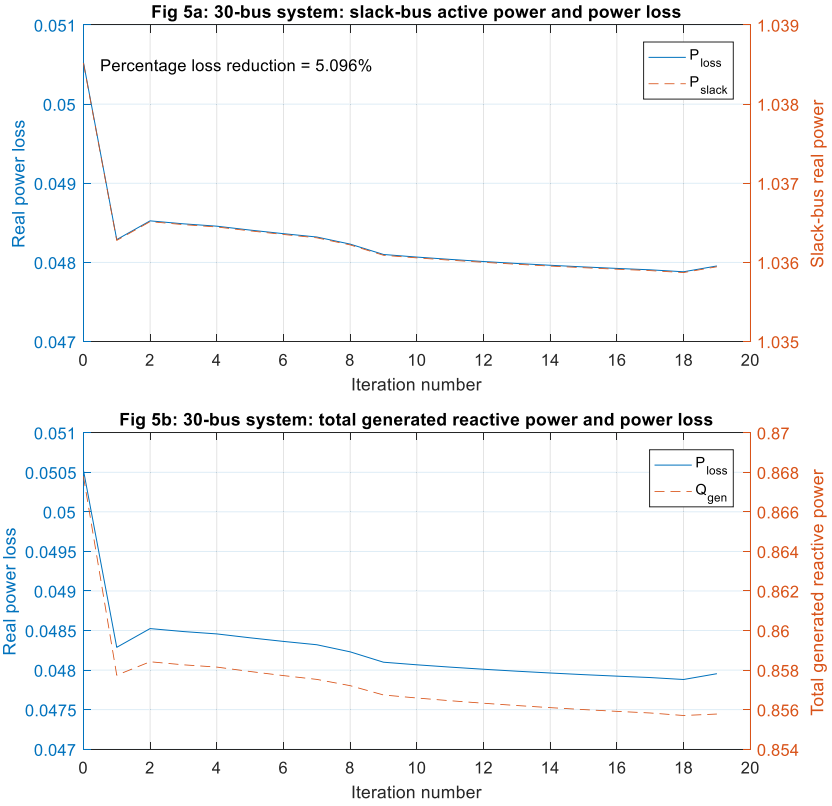

FIGURE 5. 30-bus system comparison of real power loss with slack-bus active power (5a) and with total generated reactive power (5b).

another parameter that acts as a proxy for the dual objectives of achieving optimality (i.e. making substantial advance in the Newton direction) and feasibility (i.e. improving centrality of the iterate). A value in the range $\sigma \in [0.1, 0.2]$ has been found to work well in many cases [33]. $\sigma = 0.15$ has been used in this study.

E. CHECKING CONVERGENCE OF THE ITERATES

The main criteria used for checking the convergence of the algorithm are the primal feasibility (4.32), gradient condition (4.33), objective function variation (4.34), and the barrier parameter (4.35), all of which are required to satisfy predetermined tolerances [44].

$$\max\left(\|g(x)\|_\infty, \max\left(h(x)\right)\right) \leq \varepsilon_1 \tag{4.32}$$

$$\frac{\left\|\nabla f(x) + \nabla g^T(x)\lambda_E + \nabla h^T(x)\lambda_I\right\|_\infty}{1 + \|x\|_\infty + \left\|\lambda_E\right\|_2 + \left\|\lambda_I\right\|_2} \leq \varepsilon_1 \tag{4.33}$$

$$\frac{\left|f\left(x^k\right) - f\left(x^{k-1}\right)\right|}{1 + \left|f\left(x^k\right)\right|} \leq \varepsilon_2 \tag{4.34}$$

$$\mu^k \leq \varepsilon_2 \tag{4.35}$$

Typical values for the tolerances are $\varepsilon_1 = 10^{-4}$, $\varepsilon_2 = 10^{-6}$. Besides satisfying optimality conditions as stated above, the algorithm may also terminate unsuccessfully, either due to numerical infeasibility (e.g. when the primal/dual step lengths become so small that no further progress can be made either towards reaching optimality or decreasing the barrier parameter), or the predetermined maximum number of iterations being reached before convergence of the algorithm [40].

F. PARAMETER INITIALIZATION FOR THE ALGORITHM

The primal-dual interior-point algorithm is referred to as an infeasible interior-point method, in the sense that it need not start from a feasible initial point, the only requirement being the satisfaction of the strict positivity condition on the slack variables and their corresponding dual variables [42]. In spite of this fact, initialization tends to have a significant impact on the convergence characteristics of the algorithm, and thus problem-specific heuristics are usually applied to come up with a 'good' initial point. Such a 'good' initial point should ideally be well-centered (such that values of complementarity products $s^k\lambda_I^k$ are comparable for every iteration index k), and should not be 'too infeasible' (as measured by the complementarity gap).

For the OPF problem, a candidate for the initial decision vector x^0 is the solution of a load flow computation, if available. Otherwise, a flat start may also be used, with the likelihood that the number of iterations to convergence is relatively higher [39], [42]. The slack variable vector and its corresponding dual variable vector are set as follows for

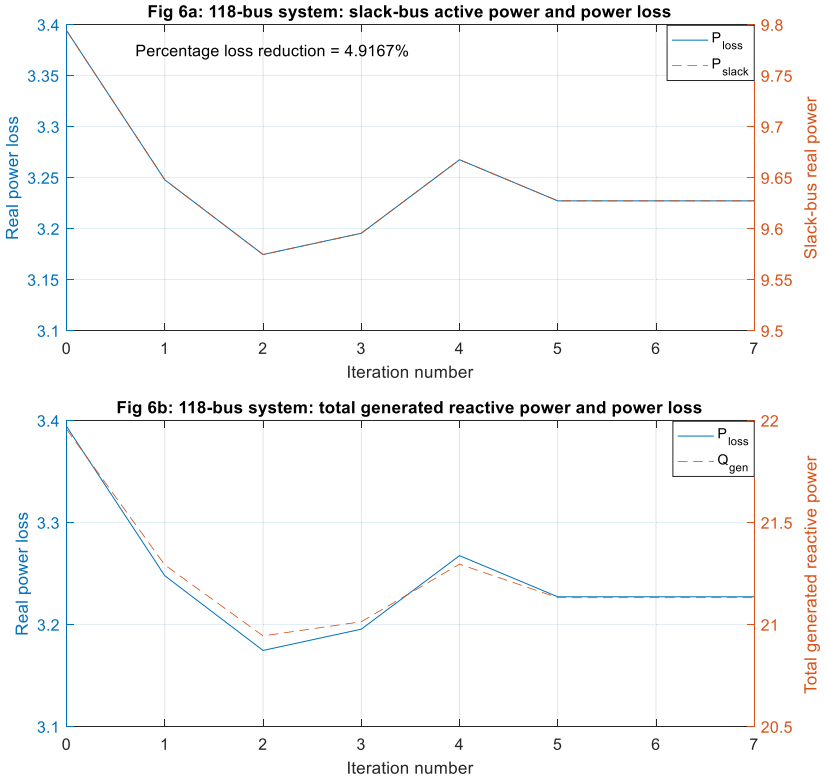

FIGURE 6. 118-bus system comparison of real power loss with slack-bus active power (6a) and with total generated reactive power (6b).

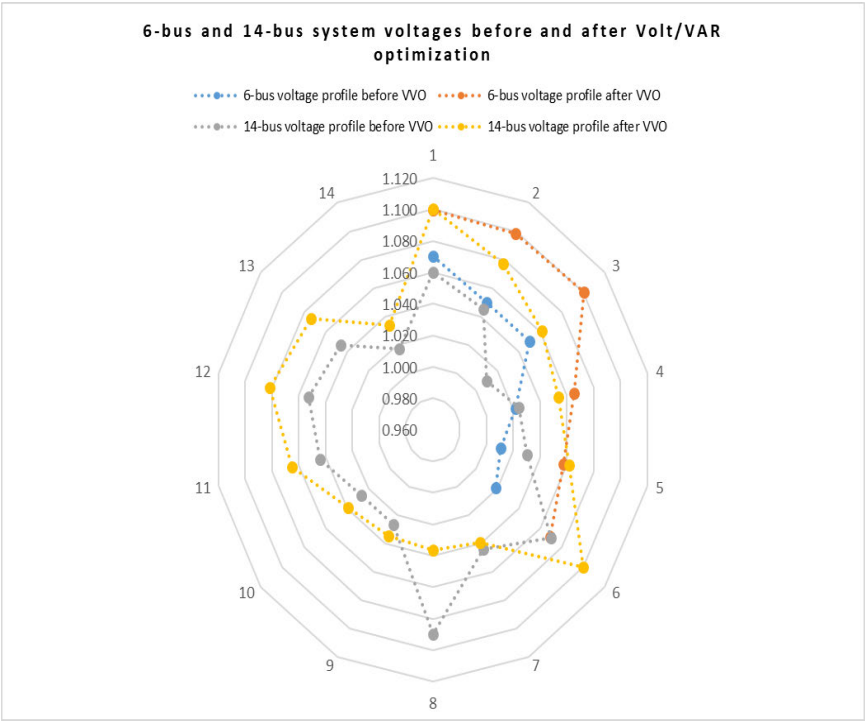

FIGURE 7. Voltage profiles of the 6-bus and 14-bus systems prior to and following Volt/VAR optimization.

the present study:

$$s^0 = \frac{1}{2}\min\left(\max\left(\mathrm{h}\left(x^0\right) - h^{\min}, h^{\max} - h\left(x^0\right)\right)\right) \tag{4.36}$$

$$\lambda_I^0 = \mu^0 \left(S^0\right)^{-1} e \tag{4.37}$$

Note that the Lagrangian multiplier vector for the equality constraints (λ_E) need not be initialized, since the design of the algorithm in this study is such that only inequality constraints are handled by the Volt/VAR optimization algorithm.

The flowchart in Fig. 2 summarizes the primal-dual interior-point method-based Volt/VAR optimization algorithm (PDIPM-VVO), as detailed in this section.

V. CASE STUDIES AND DISCUSSION OF RESULTS

A. DESCRIPTION OF THE CASE STUDIES

The designed algorithm is analysed by means of four case studies on the 6-bus, and the IEEE 14-bus, 30-bus and 118-bus test systems. The selection of the test systems enables evaluating how efficiently the algorithm scales with the system size. The performance analysis is done with particular attention paid to the following aspects:

- Magnitude of loss minimization achieved
- Voltage profile improvement due to the Volt/VAR optimization
- Efficiency and speed of convergence of the algorithm, measured by the number of iterations taken for the algorithm to converge, and the execution time
- Impact of generator reactive power output variation on both the power loss minimization and the voltage profile improvement

The algorithm is implemented in MATLAB R2022a by MathWorks Inc. [45], and tests are conducted on a computer running the Intel(R) Core(TM) i7-7700HQ CPU @ 2.80GHz, with 8,00 GB of RAM. The 6-bus case study is taken from [46]. Each of the IEEE sample systems considered in the case studies represents a portion of the transmission system in the Midwest United States, as of 1961 [47]. The data for the IEEE 14-bus and 30-bus systems is taken from [36], whereas that for the IEEE 118-bus is taken from an appendix available online, attributed to Springer Verlag [47]. The main dimensions of the test systems (i.e. number of buses, generators, lines and loads) are tabulated in Table 2.

B. ANALYSIS AND DISCUSSION OF RESULTS

The simulation results for all the case studies are summarized in Figs. 3 to 9. In Fig. 3a, the real power loss and the slack-bus active power trajectories for the 6-bus system are plotted against the iteration count of the algorithm. To account for the difference in the scale of the two quantities, a separate y-axis is used for each of the plots (but on the same set of axes). As can be observed from Fig. 3a, the real power loss and slack-bus active power trajectories actually coincide, which is expected, because any change in the system active power losses is compensated for by an equal change in the slack-bus active power output, hence the designation of "slack" bus. A real power loss reduction of 3.372% is achieved as a result of the Volt/VAR optimization. In Fig. 3b, the real power loss and total generated reactive power trajectories are plotted together against the iteration count, again using different y-axes to account for the difference in scale of the two quantities. The comparison is useful, as it reveals that the real power loss minimization objective simultaneously leads

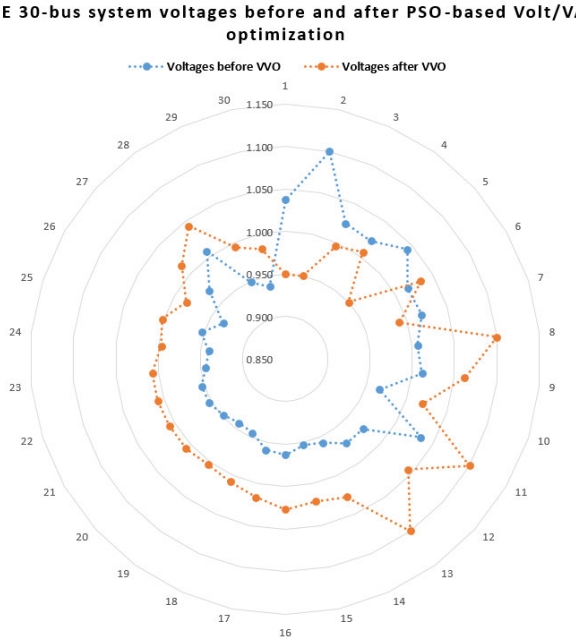

FIGURE 8. Voltage profile of the 30-bus system prior to and following Volt/VAR optimization.

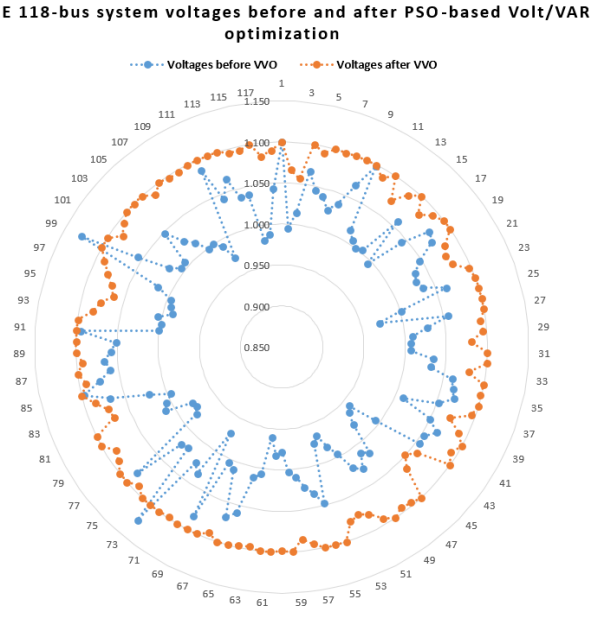

FIGURE 9. Voltage profile of the 118-bus system prior to and following Volt/VAR optimization.

TABLE 3. Performance of the PDIPM-VVO algorithm for all four test cases.

System	Number of iterations	Execution time (sec)	Initial power loss (*p.u.*)	Final power loss (*p.u.*)	Percentage loss reduction (%)
6-bus	13	0.0217	0.1335	0.1290	3.372
IEEE 14-bus	16	0.0578	0.1125	0.1047	6.914
IEEE 30-bus	20	0.2064	0.0505	0.0480	5.096
IEEE 118-bus	8	1.5723	3.3939	3.2270	4.917

TABLE 4. Performance comparison of the PDIPM-VVO algorithm presented in this article with other algorithms from the literature for the IEEE 14-bus system.

	Interior-Point Method ([36])	Linear Programming ([36])	PDIPM (presented in this article)
Initial loss (p.u.)	0.11646	0.11646	0.1125
Final loss (p.u.)	0.11004	0.11108	0.1084
% Real power loss reduction	5.513	4.619	6.914
Number of iterations	-	-	16
Execution time (sec)	18.2	61.5	0.0578

TABLE 5. Performance comparison of the PDIPM-VVO algorithm presented in this article with other algorithms from the literature for the IEEE 30-bus system.

	Modified Particle Swarm Optimization ([36])	Interior-Point Method ([36])	PDIPM (presented in this article)
Initial loss (p.u.)	-	-	0.0505
Final loss (p.u.)	0.050921	0.051109	0.0480
% Real power loss reduction	-	-	5.096
Number of iterations	-	-	20
Execution time (sec)	-	-	0.2064

to reduction in the reactive power generation in the system, which is an additional benefit of the Volt/VAR optimization.

Figs. 4 to 6 depict similar information for the IEEE 14-bus, 30-bus and 118-bus systems, respectively. Real power loss reductions can be observed for all cases, with the real power loss and slack-bus active power trajectories coinciding, and the total generated reactive power output of the system tracking the reduction in the system real power loss.

Fig. 7 depicts the pre- and post-optimization voltage profiles for the 6-bus and 14-bus systems. It can be observed that in both cases, the post-optimization voltages are higher, with only one exception in the case of the 14-bus system (specifically bus-8 voltage). Figs. 8 and 9 have similar plots for the 30-bus and 118-bus systems respectively. These two cases more clearly show improvement in the voltage profiles after optimization, particularly in terms of eliminating most of the low-voltage violations. In all cases, the bounds on the voltage magnitudes are taken to be 0.95 to 1.1 p.u. respectively, and the post-optimization voltage profiles respect these limits for all the cases.

The results of the simulations for all the cases are summarized in Table 3. Besides the percentage loss reduction, the table also lists information useful in evaluating the efficiency and scalability of the developed algorithm. The first observation that can be made is that the relationship between the number of iterations and the execution time is not strictly proportional. Thus, the 118-bus system requires the least amount of iterations to converge (8 to be precise) compared with the rest of the cases, but has the longest execution time, which is expected, since it is also of the largest size. Secondly, the algorithm also exhibits good scalability properties, in the sense that the 14-bus system requires about twice the execution time of the 6-bus system, the 30-bus system requires about three times that of the 14-bus system, and the 118-bus system has an execution time that is about seven times that of the 30-bus system. This shows that the algorithm scales quite well with the increase in the problem size. This applies at least to the studied cases, and further tests would need to be made in order to be able to state anything conclusive about such desirable performance of the algorithm.

Finally, the efficacy of the presented algorithm is demonstrated by comparing with results reported in the literature. The results are tabulated in Tables 4 and 5 for the IEEE 14-bus and IEEE-30-bus systems respectively. It can be deduced from the comparative analysis that the primal-dual interior-point algorithm presented in this article has superior performance, both in terms of solution quality (i.e. magnitude of real power loss minimization) and efficiency (i.e. required execution time).

VI. CONCLUSION AND FUTURE WORK

A detailed and thorough account of the design of a primal-dual interior-point algorithm for the Volt/VAR optimization problem formulated in rectangular coordinates has been presented in this article. The design of the algorithm

incorporates the Newton-Raphson load flow computation, also formulated in rectangular coordinates, the development of which has been presented as well. Primal-dual interior-point methods are among the most efficient classical methods for large-scale nonlinear optimization, characterized by fast convergence, and effective handling of inequality constraints. The efficiency and effectiveness of the designed algorithm has been demonstrated by means of four case studies, selected to analyse the computational efficiency and scalability of the algorithm as it is applied to systems of various sizes. Indeed, the extensive analyses that have been conducted reveal the algorithm's effectiveness and efficiency, particularly in being able to successfully solve the Volt/VAR optimization problem for systems of widely varying sizes without disproportionate increase in computational cost or deterioration in the quality of the results. Based on the case studies conducted in this article, the developed algorithm exhibits characteristics of fast convergence, high efficiency, and scalability to large-scale problems. The results obtained are very encouraging, and suggest carrying out more analyses with the goal of possibly further optimizing it so as to be able to effectively handle a wide variety of operational scenarios. The authors intend to conduct more research in this direction, which will be covered in a future article.

REFERENCES

[1] J. Carpentier, "Contribution a l'etude du dispatching economique," *Bull. de la Societé Francaise des Electriciens*, vol. 3, no. 1, pp. 431–447, 1962.

[2] F. Hasan, A. Kargarian, and A. Mohammadi, "A survey on applications of machine learning for optimal power flow," in *Proc. IEEE Texas Power Energy Conf. (TPEC)*, Feb. 2020, pp. 1–6.

[3] F. Zohrizadeh, C. Josz, M. Jin, R. Madani, J. Lavaei, and S. Sojoudi, "A survey on conic relaxations of optimal power flow problem," *Eur. J. Oper. Res.*, vol. 287, no. 2, pp. 391–409, Dec. 2020.

[4] J. K. Skolfield and A. R. Escobedo, "Operations research in optimal power flow: A guide to recent and emerging methodologies and applications," *Eur. J. Oper. Res.*, vol. 300, no. 2, pp. 387–404, Jul. 2022.

[5] B.-G. Risi, F. Riganti-Fulginei, and A. Laudani, "Modern techniques for the optimal power flow problem: State of the art," *Energies*, vol. 15, no. 17, p. 6387, Sep. 2022.

[6] P. Van Hentenryck, "Machine learning for optimal power flows," *Informs Tuts. Oper. Res.*, pp. 62–82, Oct. 2021.

[7] P. Charles, F. Mehazzem, and T. Soubdhan, "A review on optimal power flow problems: Conventional and metaheuristic solutions," in *Proc. 2nd Int. Conf. Smart Power Internet Energy Syst. (SPIES)*, Sep. 2020, pp. 577–582.

[8] E. Naderi, H. Narimani, M. Pourakbari-Kasmaei, F. V. Cerna, M. Marzband, and M. Lehtonen, "State-of-the-art of optimal active and reactive power flow: A comprehensive review from various standpoints," *Processes*, vol. 9, no. 8, p. 1319, Jul. 2021.

[9] I. A. Zorin and E. N. Gryazina, "An overview of semidefinite relaxations for optimal power flow problem," *Autom. Remote Control*, vol. 80, no. 5, pp. 813–833, May 2019.

[10] S. Frank, I. Steponavice, and S. Rebennack, "Optimal power flow: A bibliographic survey I: Formulations and deterministic methods," *Energy Syst.*, vol. 3, no. 3, pp. 221–258, Sep. 2012.

[11] S. Krishnamurthy and R. Tzoneva, "Investigation of the methods for single area and multi area optimization of a power system dispatch problem," *Int. Rev. Electr. Eng.*, vol. 7, no. 1, pp. 3600–3627, Jan./Feb. 2012.

[12] K. S. Pandya and S. K. Joshi, "A survey of optimal power flow methods," *J. Theor. Appl. Inf. Technol.*, vol. 4, no. 5, pp. 452–458, May 2008.

[13] J. A. Momoh, M. E. El-Harway, and R. Adapa, "A review of selected optimal power flow literature to 1993. II. Newton, linear programming and interior point methods," *IEEE Trans. Power Syst.*, vol. 14, no. 1, pp. 96–111, Feb. 1999.

[14] M. Huneault and F. D. Galiana, "A survey of the optimal power flow literature," *IEEE Trans. Power Syst.*, vol. 6, no. 2, pp. 762–770, May 1991.

[15] O. Alsac, J. Bright, M. Paris, and B. Stott, "Further developments in LP-based optimal power flow," *IEEE Trans. Power Syst.*, vol. 5, no. 3, pp. 697–711, Aug. 1990.

[16] H. H. Happ, "Optimal power dispatch: A comprehensive survey," *IEEE Trans. Power App. Syst.*, vol. PAS-90, no. 3, pp. 841–854, May 1977.

[17] H. W. Dommel and W. F. Tinney, "Optimal power flow solutions," *IEEE Trans. Power App. Syst.*, vol. PAS-87, no. 10, pp. 1866–1876, Oct. 1968.

[18] J. Peschon, D. Piercy, W. Tinney, O. Tveit, and M. Cuenod, "Optimum control of reactive power flow," *IEEE Trans. Power App. Syst.*, vol. PAS-87, no. 1, pp. 40–48, Jan. 1968.

[19] I. Hano, Y. Tamura, S. Narita, and K. Matsumoto, "Real time control of system voltage and reactive power," *IEEE Trans. Power App. Syst.*, vol. PAS-88, no. 10, pp. 1544–1559, Oct. 1969.

[20] H. Mataifa, S. Krishnamurthy, and C. Kriger, "Volt/VAR optimization: A survey of classical and heuristic optimization methods," *IEEE Access*, vol. 10, pp. 13379–13399, 2022.

[21] D. Sun, B. Ashley, B. Brewer, A. Hughes, and W. Tinney, "Optimal power flow by Newton approach," *IEEE Trans. Power App. Syst.*, vol. PAS-103, no. 10, pp. 2864–2880, Oct. 1984.

[22] K. R. Frisch, "The logarithmic potential method of convex programming," Univ. Inst. Econ., Oslo, Norway, Tech. Memorandum, May 1955.

[23] A. V. Fiacco and G. P. McCormick, *Nonlinear Programming: Sequential Unconstrained Minimization Techniques*. Hoboken, NJ, USA: Wiley, 1968.

[24] N. Karmarkar, "A new polynomial-time algorithm for linear programming," *Combinatorica*, vol. 4, pp. 373–395, 1984.

[25] A. Forsgren, P. E. Gill, and M. H. Wright, "Interior methods for nonlinear optimization," *SIAM Rev.*, vol. 44, no. 4, pp. 525–597, Apr. 2002.

[26] A. M. Chebbo, M. R. Irving, and M. J. H. Sterling, "Reactive power dispatch incorporating voltage stability," *IEE Proc. C, Gener., Transmiss. Distrib.*, vol. 139, no. 3, p. 253, 1992.

[27] T. J. E. Miller, *Reactive Power Control in Electric Systems*. Hoboken, NJ, USA: Wiley, 1982.

[28] J. A. Momoh, *Electric Power System Applications of Optimization*. New York, NY, USA: Marcel Dekker, 2001.

[29] A. M. Chebbo, "Security constrained reactive power dispatch in electrical power systems," Ph.D. dissertation, School Eng. Appl. Sci., Durham Univ., Durham, U.K., 1990.

[30] P. Kundur, *Power System Stability and Control*. New York, NY, USA: McGraw-Hill, 1994.

[31] A. Rabiee and M. Parniani, "Voltage security constrained multi-period optimal reactive power flow using benders and optimality condition decompositions," *IEEE Trans. Power Syst.*, vol. 28, no. 2, pp. 696–708, May 2013.

[32] F. Capitanescu, M. Glavic, and L. Wehenkel, "An interior point method based optimal power flow," in *Proc. 3rd ACOMEN Conf.*, Ghent, Belgium, Jun. 2005, pp. 1–18.

[33] G. L. Torres and V. H. Quintana, "An interior-point method for nonlinear optimal power flow using voltage rectangular coordinates," *IEEE Trans. Power Syst.*, vol. 13, no. 4, pp. 1211–1218, Nov. 1998.

[34] N. Deeb and S. M. Shahidehpour, "Linear reactive power optimization in a large power network using the decomposition approach," *IEEE Trans. Power Syst.*, vol. 5, no. 2, pp. 428–438, May 1990.

[35] M. Albadi, "Power flow analysis," in *Computational Models in Engineering*. London, U.K.: IntechOpen, 2019.

[36] J. Zhu, *Optimization of Power System Operation*. Hoboken, NJ, USA: Wiley, 2009.

[37] J. D. Glover and M. S. Sarma, *Power System Analysis and Design*, 3rd ed. Belmont, CA, USA: Wadsworth, 2002.

[38] A. J. Wood, B. F. Wollenberg, and G. B. Sheble, *Power Generation, Operation and Control*, 3rd ed. Hoboken, NJ, USA: Wiley, 2014.

[39] J. L. M. Ramos, A. G. Exposito, and V. H. Quintana, "Transmission power loss reduction by interior-point methods: Implementation issues and practical experience," *IEE Proc., Gener., Transmiss. Distrib.*, vol. 152, no. 1, p. 90, 2005.

[40] R. D. Zimmerman and C. Murillo-Sanchez. *MATPOWER User's Manual*. [Online]. Available: http://www.pserc.cornell.edu/matpower/

[41] J. Nocedal and S. J. Wright, *Numerical Optimization*, 2nd ed. New York, NY, USA: Springer, 2006.

[42] G. L. Torres, "Nonlinear optimal power flow by interior and non-interior point methods," Ph.D. dissertation, Dept. Elect. Eng., Univ. Waterloo, Waterloo, ON, Canada, 1998.
[43] S. J. Wright, *Primal-Dual Interior-Point Methods*. Philadelphia, PA, USA: Society for Industrial and Applied Mathematics, 1997.
[44] F. Capitanescu, M. Glavic, D. Ernst, and L. Wehenkel, "Interior-point based algorithms for the solution of optimal power flow problems," *Electr. Power Syst. Res.*, vol. 77, nos. 5–6, pp. 508–517, Apr. 2007.
[45] *MATLAB, Version R2022a*, MathWorks, Natick, MA, USA, 2022.
[46] F. M. Gonzalez-Longatt. (2015). *IEEE 14 Bus Test*. Accessed: Aug. 30, 2022. [Online]. Available: https://www.fglongatt.org/Test_Systems/IEEE_14bus.html
[47] Springer Verlag. (2012). *Appendix E: IEEE 118-Bus Test System Data*. Accessed: May 5, 2022. [Online]. Available: https://link.springer.com/content/pdf/bbm%3A978-1-4615-4473-9%2F1.pdf

H. MATAIFA received the B.Tech. and M.Tech. degrees in electrical engineering from the Cape Peninsula University of Technology (CPUT), Cape Town, South Africa, in 2011 and 2016, respectively, and the B.Sc. degree in applied mathematics and computer science from the University of South Africa (UNISA), in 2020. He is currently pursuing the Ph.D. degree in electrical engineering with the Department of Electrical, Electronic and Computer Engineering (DEECE), CPUT. From 2012 to 2017, he was a Research Assistant with the Centre for Substation Automation and Energy Management Systems (CSAEMS), CPUT, where he has been a Lecturer with the Electrical Engineering Department, since 2018. His research interests include the optimization of power system operation and efficient grid integration of distributed energy resource technologies.

S. KRISHNAMURTHY (Member, IEEE) received the B.Eng. and M.Eng. degrees in power systems from Annamalai University, India, in 2006 and 2008, respectively, and the Doctorate of Technology degree in electrical engineering from the Cape Peninsula University of Technology (CPUT), Cape Town, South Africa, in 2013.

He has been a Senior Lecturer with the Department of Electrical, Electronic and Computer Engineering, CPUT, since 2013. He currently heads the Cluster of Power Systems. He is the Deputy Leader of the Centre for Substation Automation and Energy Management Systems (CSAEMS), supported by the National Research Foundation (NRF). He has received several industrial grants, among them the ESKOM TESP and EPPEI Projects. His research interests include power systems, protective relaying systems, substation automation, renewable energy, energy management systems, and parallel computing. He is a member of the Institute of Engineers in India (IEI) and the South African Institute of Electrical Engineers (SAIEE). He is a registered Professional Engineer with the Engineering Council of South Africa (ECSA).

C. KRIGER received the B.Eng. degree from Saxion Hogeschole Enschede, The Netherlands, and the B.Tech., M.Tech., and Doctorate of Engineering degrees from the Cape Peninsula University of Technology (CPUT), Cape Town, South Africa.

He is currently a Senior Lecturer with the Department of Electrical, Electronic and Computer Engineering, CPUT, where he also heads the Centre for Substation Automation and Energy Management Systems (CSAEMS). He has completed numerous industrial projects and has worked with the automotive vehicle industry, with a focus on the design, testing, and commissioning of electronic systems. He has conducted diverse industrial research projects encompassing the testing of the chemical composition of vehicle emissions, modeling, simulation, and implementation of wastewater systems, and in the field of substation automation, the development of IEC61850 standard-based object models for condition monitoring and application to induction motors, embedded system implementation, GOOSE and sampled value message investigations, protection, automation, control, and neural networks application to condition monitoring. His research interests include modeling and simulation of control systems, energy management systems, substation automation, image processing, neural networks, and condition monitoring. He is a Candidate Member of the Institute for Professional Technologists.